International Journal of Nanomedicine

Dovepress
open access to scientific and medical research

Open Access Full Text Article

ORIGINAL RESEARCH

Kalopanacis Cortex extract-capped gold nanoparticles activate NRF2 signaling and ameliorate damage in human neuronal SH-SY5Y cells exposed to oxygen–glucose deprivation and reoxygenation

This article was published in the following Dove Press journal:
International Journal of Nanomedicine
22 June 2017
Number of times this article has been viewed

Sun Young Park[1]
Seon Yeong Chae[1,2]
Jin Oh Park[2]
Kyu Jin Lee[2]
Geuntae Park[1,2]

[1]Bio-IT Fusion Technology Research Institute, [2]Department of Nanofusion Technology, Graduate School, Pusan National University, Busan, Republic of Korea

Abstract: Recently, environment-friendly synthesis of gold nanoparticles (GNPs) has been extensively explored by biologists and chemists. However, significant research is still required to determine whether "eco-friendly" GNPs are beneficial to human health and to elucidate the molecular mechanisms of their effects on human cells. We used human neuronal SH-SY5Y cells to show that treatment with Kalopanacis Cortex extract-capped GNPs (KC-GNs), prepared via an eco-friendly, fast, one-pot synthetic route, protected neuronal cells against oxygen–glucose deprivation/reoxygenation (OGD/R)-induced damage. To prepare GNPs, Kalopanacis Cortex was used without any chemical reducing and stabilizing agents. Ultraviolet–visible spectroscopy showed maximum absorbance at 526 nm owing to KC-GN surface plasmon resonance. Hydrodynamic size (54.02±2.19 nm) and zeta potential (–20.3±0.04 mV) were determined by dynamic light scattering. The average diameter (41.07±3.05 nm) was determined by high-resolution transmission electron microscopy. Energy-dispersive X-ray diffraction spectroscopy and X-ray diffraction confirmed the presence of assembled GNPs. Fourier transform infrared analysis suggested that functional groups such as O–H, C–C, and C–N participated in KC-GN formation. Cell viability assays indicated that KC-GNs restored the viability of OGD/R-treated SH-SY5Y cells. Flow cytometry demonstrated that KC-GNs inhibited the OGD/R-induced reactive oxygen species production and mitochondrial membrane potential disruption. KC-GNs also inhibited the apoptosis of OGD/R-exposed cells. Western blot analysis indicated that the OGD/R-induced cellular apoptosis and simultaneous increases in the expression of cleaved caspase-3, p53, p21, and B-cell lymphoma 2-associated X protein were reversed by KC-GNs. The KC-GN-mediated protection against OGD/R-induced neurotoxicity was diminished by NRF2 and heme oxygenase-1 gene knockdowns. Collectively, these results suggested that KC-GNs exerted strong neuroprotective effects on human neuronal cells, which might be attributed to the attenuation of OGD/R-induced neuronal cell injury through the NRF2 signaling pathway.

Keywords: gold nanoparticle, Kalopanacis Cortex, oxygen–glucose deprivation, neuroprotection, NRF2

Correspondence: Geuntae Park
Department of Nanofusion Technology, Graduate School, Pusan National University, Busan 609-735, Republic of Korea
Tel +82 51 510 3740
Fax +82 51 518 4113
Email gtpark@pusan.ac.kr

Introduction

Cerebral ischemia or stroke is one of the most frequent causes of death and disability in elderly populations worldwide. It is characterized by blood vessel occlusion, which

submit your manuscript | www.dovepress.com
Dovepress
http://dx.doi.org/10.2147/IJN.S138178

results in the deficiency of oxygen and nutrient supplies to the brain and leads to neuronal injury.[1] The treatment for blood vessel occlusion commonly involves reperfusion, which is rapid restoration of the blood flow. Although reperfusion is critical for ensuring normal functioning of the cerebral ischemic brain, it can, paradoxically, lead to secondary brain damage, which is referred to as ischemia–reperfusion injury (IRI).[2] The primary factor in the initiation of the pathological response to IRI is oxidative stress-induced damage in a brain region, caused by the absence of oxygen and glucose. Other impaired processes include mitochondrial metabolism, regulation of pro- and anti-apoptotic factors, and neurological processes.[3] The current therapeutic approaches largely rely on pharmacological and mechanical thrombolysis, but their therapeutic effects are limited. A regular supply of oxygen and glucose plays a critical role in the regulation of normal neuronal function. Recent studies have shown that oxygen–glucose deprivation/reperfusion (OGD/R), an in vitro model that mimics the fundamental aspects of ischemic injury, is a multifaceted process with complex mechanisms involving oxidative stress, mitochondrial dysfunction, apoptosis, and regulation of gene expression, which ultimately trigger neuronal cell death and brain damage.[4–6]

It has been suggested that oxidative stress is a major contributor to neuronal dysfunction and one of the main causes of ischemic injury. Oxidative stress is due to an imbalance between pro- and antioxidants, and results in the excessive production of reactive oxygen species (ROS).[7,8] The brain has a highly developed endogenous antioxidant defense system to counteract the oxidative stress generated by neuronal damage. Antioxidant response element (ARE)-regulated Phase II detoxifying enzymes are the principal means by which neuronal cells protect themselves from excessive production of ROS.[9] A master regulator of these specific antioxidant Phase II enzymes is the transcription factor NRF2. NRF2 is accumulated in the nucleus and coordinates the expression of antioxidant Phase II enzymes through the initiation of transactivation. Activation of NRF2 is a key step in endogenous neuronal cell protection and has been demonstrated to be a promising therapeutic target for neuroprotection.[10] Numerous studies have demonstrated that the NRF2 antioxidant response signaling pathway offers neuroprotection against cerebral IRI.[9,11] Drugs that activate the NRF2/ARE pathway and related antioxidant phase II enzymes would, therefore, present a promising neuroprotective treatment for ischemic injury.[12] Although responses of the NRF2 signaling pathway to gold nanoparticles (GNPs) have been investigated,[13–15] no studies have been performed to determine the role of NRF2 signaling in the neuroprotective response to OGD/R-mediated neuronal cell injury.

Nanotechnology has a great potential for biomedical applications, nutrition, and cosmetics, owing to novel properties of nanomaterials, which are different from those of isolated atoms and bulk materials.[16,17] Much attention has been paid to the manufacture of novel nanoparticles without the use of harmful chemicals to eliminate the potential hazards for pharmaceutical, cosmetic, and biomedical applications.[18] Hence, a major challenge for scientists is the use of biological components as nontoxic and eco-friendly sources for the development of GNPs with broad biomedical applications. To avoid harmful chemicals, medicinal plant-mediated synthesis is preferred, owing to its rapid, direct reaction and accumulation of bioactive phytonutrients that may provide biologically active GNPs for diagnosis and treatment purposes.[19,20] Gold has been extensively used in nervines, herb medicines that can improve symptoms in patients with nervous conditions, and several nanomaterials have emerged as improved therapies for the prevention and treatment of neuronal injury. Therefore, we focused on Kalopanacis Cortex (KC), a dried stem bark of *Kalopanax pictus*, which has been mainly used for the treatment of neuralgia, lumbago, furuncles, wounds, rheumatoid arthritis, and diabetes mellitus.[21,22] Studies have revealed that the major constituents of this plant are saponins, polyacetylenes, phenylpropanoid glycosides, lignans, and simple phenolic glycosides.[23,24] The bioactive compounds of KC have been reported to have diverse effects, such as anti-inflammatory, antitumor, antioxidant, and antibacterial activities.

This study is the first to test KC in the green synthesis to produce GNPs for biomedical applications. The synthesized Kalopanacis Cortex extract-capped GNPs (KC-GNs) were extensively characterized by spectroscopic and analytical techniques, including ultraviolet–visible (UV–Vis) spectroscopy, dynamic light scattering (DLS), field emission transmission electron microscopy (TEM), energy-dispersive X-ray spectroscopy (EDS), elemental mapping, X-ray diffraction (XRD), and Fourier transform infrared (FTIR) spectroscopy. Using a cellular model of OGD/R, we aimed to examine the potential role of KC-GNs in neuronal survival. We found that KC-GNs significantly attenuated the apoptosis of human neuronal cells exposed to OGD/R treatment and significantly inhibited the OGD/R-induced ROS production and mitochondrial dysfunction in human neuronal cells. Furthermore, RNA silencing of NRF2 significantly blocked the neuroprotective effects of KC-GNs against OGD/R-induced injury. Thus, our

study suggested that KC-GNs protected neurons against OGD/R-induced injury via NRF2 signaling.

Materials and methods

Materials and chemicals

A lactate dehydrogenase (LDH) assay kit for cytotoxicity detection was purchased from Roche Applied Science (Risch-Rotkreuz, Switzerland). The APO-BrdU™ TUNEL assay kit was purchased from Thermo Fisher Scientific (Waltham, MA, USA). Nuclear and Cytoplasmic Extraction Reagents (NE-PER) nuclear and cytoplasmic extraction reagents, a chloromethyl derivative of 2′,7′-dichlorodihydrofluorescein diacetate (CM-H_2DCFDA), and the MitoProbe™ JC-1 assay kit for flow cytometry were purchased from Thermo Fisher Scientific. Dulbecco's Modified Eagle's Medium (DMEM) and fetal bovine serum (FBS) were purchased from Thermo Fisher Scientific. Gold chloride trihydrate, 3-[4,5-dimethylthiazol-2-yl]-2,5-diphenyltetrazolium bromide (MTT), and other reagents were purchased from Sigma-Aldrich Co. (St Louis, MO, USA). Small interfering RNAs (siRNAs) against NRF2 and NAD(P)H quinone dehydrogenase 1 (NQO1) and antibodies against α-tubulin, TATA-binding protein (TBP), NRF2, heme oxygenase-1 (HO-1), and NQO1 were purchased from Santa Cruz Biotechnology Inc. (Dallas, TX, USA). Cleaved caspase-3, a cleaved caspase-3 (Asp175)–Alexa Fluor® 488 antibody conjugate, p53, and p21 were purchased from Cell Signaling Technology (Beverly, MA, USA). The FuGENE HD transfection reagent and X-tremeGENE siRNA transfection reagent were obtained from Hoffmann-La Roche Ltd. (Basel, Switzerland).

Preparation of KC extract

KC (the stem bark of *K. pictus*) was purchased from a local herb store, Kwang Myoung Herb Medicine (Pusan, Korea), in April 2005. The roots were identified and authenticated by Professor WS Ko, College of Oriental Medicine, Dong-eui University, Pusan, Korea. A voucher specimen (KP-05-04) was deposited at the Department of Molecular Biology, Pusan National University, Busan, Korea. Dry roots (300 g) were extracted using distilled water at 100°C for 4 h. The extract was filtered through a 0.45-μm filter, freeze-dried (yield =27 g), and stored at 4°C. The dried extract was dissolved in phosphate-buffered saline (PBS) and filtered through a 0.22-μm filter before use.

Green synthesis of KC-GNs

KC-GNs were prepared by the reduction method using chloroauric acid in accordance with a previously described protocol[25] with slight modifications. In the biological synthesis of KC-GNs, a mixture of a 1 mM $HAuCl_4$ solution and the KC extract was incubated for 15 min at 200 rpm and 25°C. The undesirable components were separated by centrifugation at 13,000 rpm for 20 min and washed three times with deionized water to remove the remaining residues. Finally, the purified KC-GNs were confirmed by UV–Vis spectrophotometry using an Ultrospec 6300 Pro (GE Healthcare Life Sciences, Buckinghamshire, UK) at wavelengths in the range from 300 to 800 nm. The nanoparticle size and zeta potential were measured by DLS using the Data Transfer Assistance software and a Zetasizer Nano ZS90 (Malvern Instruments, Malvern, UK).

TEM and EDS

The synthesized KC-GNs were placed on a carbon-coated copper grid, dried, and then analyzed. Images from a 200-kV field emission transmission electron microscope (TALOS F200X; FEI, Hillsboro, OR, USA) were used to determine the shape and size of the synthesized KC-GNs. High-resolution images were acquired to provide better quality TEM data. The selected area electron diffraction (SAED) pattern of KC-GNs was consistent with the high-resolution transmission electron microscopy (HR-TEM) data, which confirmed the crystalline nature of the synthesized KC-GNs. The composition of KC-GNs was analyzed using the TEM instrument equipped with an energy-dispersive X-ray spectroscope.

XRD and FTIR spectroscopy

Structural characteristics of the KC extract and KC-GNs were analyzed by XRD and FTIR methods. To confirm the crystalline structure, the KC extract and KC-GNs were freeze-dried and analyzed using an X-ray diffractometer (XRD Empyrean Series 2; PANalytical, Almelo, the Netherlands). The XRD pattern was determined with the following parameters: scanning range, 30–80; voltage, 40 kV; and current, 30 mA. FTIR spectra of the KC extract and KC-GNs were recorded on an FTIR spectrophotometer (Spectrum GX; PerkinElmer, Inc., Waltham, MA, USA) using KBr pellets in the range from 4,000 to 400 cm^{-1}. FTIR analysis was conducted to identify various functional groups and the formation of GNPs.

Cell culture

SH-SY5Y cells, a human-derived neuroblastoma cell line, were obtained from the American Type Culture Collection (Manassas, VA, USA) and grown as monolayers in DMEM supplemented with 10% heat-inactivated FBS. SH-SY5Y

cells were incubated at 37°C in a humidified atmosphere containing 5% CO_2. To avoid changes in cell characteristics, caused by extended culture, all experiments were conducted with cells between passages 15 and 25. To maintain exponential growth, each cell culture was subcultured every 3 days using trypsin/ethylenediaminetetraacetic acid treatment.

Oxygen–glucose deprivation and reoxygenation

To establish an in vitro ischemic injury model, SH-SY5Y cells were washed twice with pre-warmed PBS and then incubated in glucose- and serum-free DMEM containing nanoparticle formulations in an anaerobic humidified chamber filled with 1% O_2, 95% N_2, and 5% CO_2 for 8 h at 37°C. The cells were then cultured in a normal medium under normoxic conditions for 24 h. Normoxic cells without OGD were maintained in a complete medium under normoxic conditions for 8 h at 37°C in an atmosphere of 95% air and 5% CO_2.

Cell viability and cytotoxicity assays

An MTT solution (50 μg/mL) was added to each well, and the plates were incubated for 6 h at 37°C in an atmosphere of 5% CO_2, followed by supernatant removal. The formazan crystals formed in viable cells were solubilized with dimethyl sulfoxide. Absorbance was measured in each well at 570 nm using a microplate reader (Wallac 1420; PerkinElmer, Inc.). Extracellular LDH activity was measured using a cytotoxicity detection kit in accordance with the manufacturer's protocol. Absorbance was measured in each well at 490 nm using a microplate reader (Wallac 1420).

Measurement of intracellular ROS

To evaluate the levels of intracellular ROS, cells were treated with CM-H_2DCFDA for 1 h at 37°C in an atmosphere of 5% CO_2, then harvested, and washed three times with PBS. Fluorescence intensity was then measured by flow cytometry at an excitation wavelength of 488 nm and an emission wavelength of 525 nm. Data analyses were performed using the CXP software 2.0 (Beckman Coulter, Pasadena, CA, USA).

Terminal deoxynucleotidyl transferase dUTP nick end labeling assay

Cells were evaluated using a terminal deoxynucleotidyl transferase dUTP nick end labeling (TUNEL) assay with the APO-BrdU™ TUNEL assay kit in accordance with the manufacturer's instructions. The results were analyzed by flow cytometry (fluorescein isothiocyanate; excitation at 488 nm and emission at 520 nm). Data analyses were performed using CXP software 2.0.

Mitochondrial membrane potential assay

To determine the mitochondrial membrane potential, cells were stained with the MitoProbe™ JC-1 assay kit and subsequently analyzed by flow cytometry with the CXP software 2.0. For each sample, 10,000 cells were acquired, and the fluorescence intensity of the cell population was analyzed.

Protein extraction and Western blot analysis

Cytosolic and nuclear extracts were isolated using NE-PER nuclear and cytoplasmic extraction reagents in accordance with the manufacturer's instructions. The protein content of cell lysates was determined using the Bradford reagent (Bio-Rad Laboratories Inc., Hercules, CA, USA). Proteins were separated by sodium dodecyl sulfate polyacrylamide gel electrophoresis and transferred to a polyvinylidene difluoride membrane. Membranes were incubated with an appropriate primary antibody and then with a horseradish peroxidase-conjugated anti-rabbit or anti-mouse secondary antibody. The bound secondary antibodies were visualized using an enhanced chemiluminescence detection system (Amersham Biosciences, Piscataway, NJ, USA), and images were acquired using an ImageQuant 350 analyzer (Amersham Biosciences).

Transient transfection and dual-luciferase assay

Cells were transfected with ARE reporter plasmids or an HO-1 promoter reporter plasmid using the FuGENE HD reagent in accordance with the manufacturer's instructions. A *Renilla* luciferase control plasmid, pRL-CMV, was cotransfected as an internal control for transfection efficiency. Luciferase activity was assayed using a dual-luciferase assay kit in accordance with the manufacturer's instructions. Luminescence was measured using a microplate luminometer (Wallac 1420).

Transient transfection with siRNAs

siRNAs were transfected into cells using the X-tremeGENE siRNA transfection reagent (Roche Applied Science) in accordance with the manufacturer's instructions. Commercially available mouse NRF2- and HO-1-specific siRNAs and negative control siRNAs were used for the transfection. Briefly, the X-tremeGENE siRNA transfection reagent was added to a

serum-free medium containing each siRNA and incubated for 20 min at room temperature. Cells were transfected with the control siRNA, siRNA targeting NRF2, or siRNA targeting HO-1. At 24 h after the transfection, the cells were treated with KC-GNs for 1 h and then stimulated with OGD/R.

Statistical analysis

Data were expressed as the mean ± standard error of the mean. Statistical analysis was performed using the Statistical Package for the Social Sciences (SPSS) software (Version 18.0, Chicago, IL, USA) to identify significant differences based on one-way analysis of variance, followed by Dunn's post hoc tests. Values of $P<0.05$ were considered statistically significant. Each experiment was repeated a minimum of three times.

Results

Characterization of synthesized KC-GNs

UV–Vis spectral analysis is a common method used to determine the formation of metal nanoparticles. Addition of the KC extract to $HAuCl_4$ resulted in a change in color from yellow to ruby red within 15 min at room temperature, confirming the formation of KC-GNs. The UV–Vis absorption spectra of the KC extract and synthesized KC-GNs were recorded from 300 to 800 nm. The spectrum of the KC extract showed no peaks, but that of KC-GNs showed a characteristic absorption peak at a wavelength of ~526 nm, which was attributed to the surface plasmon resonance (SPR; Figure 1A and B). DLS analysis was performed to identify the hydrodynamic size distribution of KC-GNs in solution. A qualitative DLS image showing the size distribution of KC-GNs is shown in Figure 1C. The average particle size of KC-GNs was 54.02±2.19 nm, and the zeta potential was –20.3±0.04 mV, which indicated the presence of a repulsive force for electrostatic stabilization (Figure 1D).

TEM and EDS analyses of synthesized KC-GNs

The morphology, shape, and size of the synthesized KC-GNs were analyzed using HR-TEM. In the HR-TEM images, the synthesized KC-GNs were approximately spherical or hexagonal with lattice fringes and were ~41.07±3.05 nm, owing to the strong reducing nature and capping agents of the KC extract (Figure 2A–C). The SAED pattern indicated

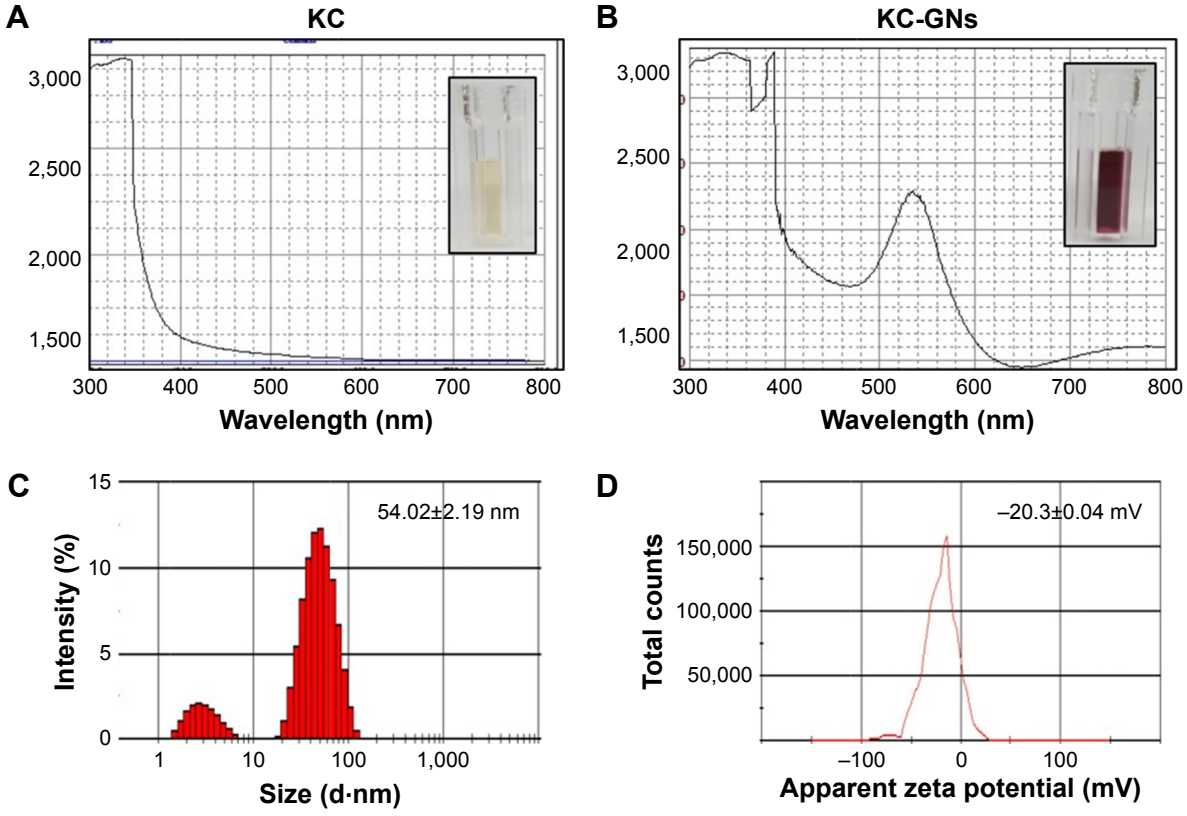

Figure 1 Synthesis and characterization of KC-GNs.
Notes: UV–Vis spectroscopic analysis of the KC extract (**A**) and synthesized KC-GNs (**B**). The hydrodynamic size (**C**) and zeta potential (**D**) of the synthesized KC-GNs were determined by DLS.
Abbreviations: DLS, dynamic light scattering; KC, Kalopanacis Cortex; KC-GN, Kalopanacis Cortex extract-capped gold nanoparticle; UV–Vis, ultraviolet–visible.

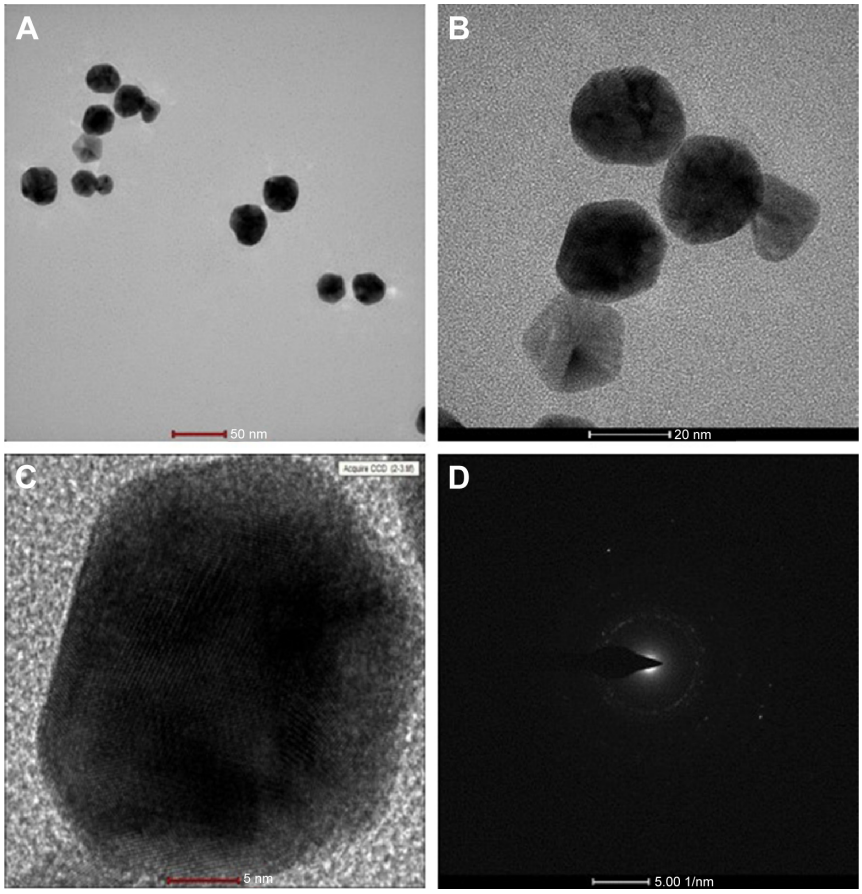

Figure 2 HR-TEM images of synthesized KC-GNs.
Notes: (**A**–**C**) Morphology of the synthesized KC-GNs was confirmed by low- and high-magnification images and HR-TEM images. (**D**) The SAED pattern of the synthesized KC-GNs was obtained by HR-TEM.
Abbreviations: HR-TEM, high-resolution transmission electron microscopy; KC-GN, Kalopanacis Cortex extract–gold nanoparticle; SAED, selected area electron diffraction.

the crystalline metallic nature of the synthesized KC-GNs (Figure 2D). The energy-dispersive spectra of the synthesized KC-GNs, analyzed by EDS, indicated the presence of elemental gold; thus, the bioreduced nanoparticles formed upon using KC in the synthesis contained elemental gold (Figure 3).

XRD and FTIR analyses of synthesized KC-GNs

The crystalline nature of the synthesized KC-GNs was confirmed by XRD analysis. The XRD pattern of the synthesized KC-GNs showed that these GNPs, unlike the KC extract, had a crystalline structure (Figure 4A). The Bragg reflection peaks at 2θ=37.77°, 43.74°, 64.50°, and 77.33° corresponded to the (111), (200), (220), and (311) planes, respectively (Figure 4B). Therefore, the synthesized KC-GNs had a face-centered cubic (FCC) structure. FTIR spectroscopy provided information on various functional groups that were present on the surface of the synthesized KC-GNs and their chemical changes. The FTIR spectra of the KC extract and KC-GNs were recorded and are shown in Figure 4C. The intense peaks in the FTIR spectra of both KC and KC-GNs, located at 3,411 and 3,409 cm^{-1}, corresponded to O–H stretching of alcohols and phenolic compounds, respectively; those at 1,619 and 1,642 cm^{-1} or 1,449 and 1,512 cm^{-1} corresponded to C–C stretching of aromatic groups; and those at 1,076 and 1,118 cm^{-1} corresponded to C–N stretching of aliphatic amine groups.

KC-GNs protect human neuronal cells against OGD/R-stimulated cytotoxicity

To examine the time dependency of OGD in SH-SY5Y cells, the cells were transiently exposed to OGD for different times (2, 4, 8, 12, and 16 h) and then reoxygenated for 24 h and evaluated using the MTT and LDH assays. The MTT assay results showed that the viability of the OGD/R-exposed cells decreased in a time-dependent manner. Meanwhile, the LDH activity increased in a time-dependent manner (Figure 5A and B). Based on the data, the OGD/R treatment

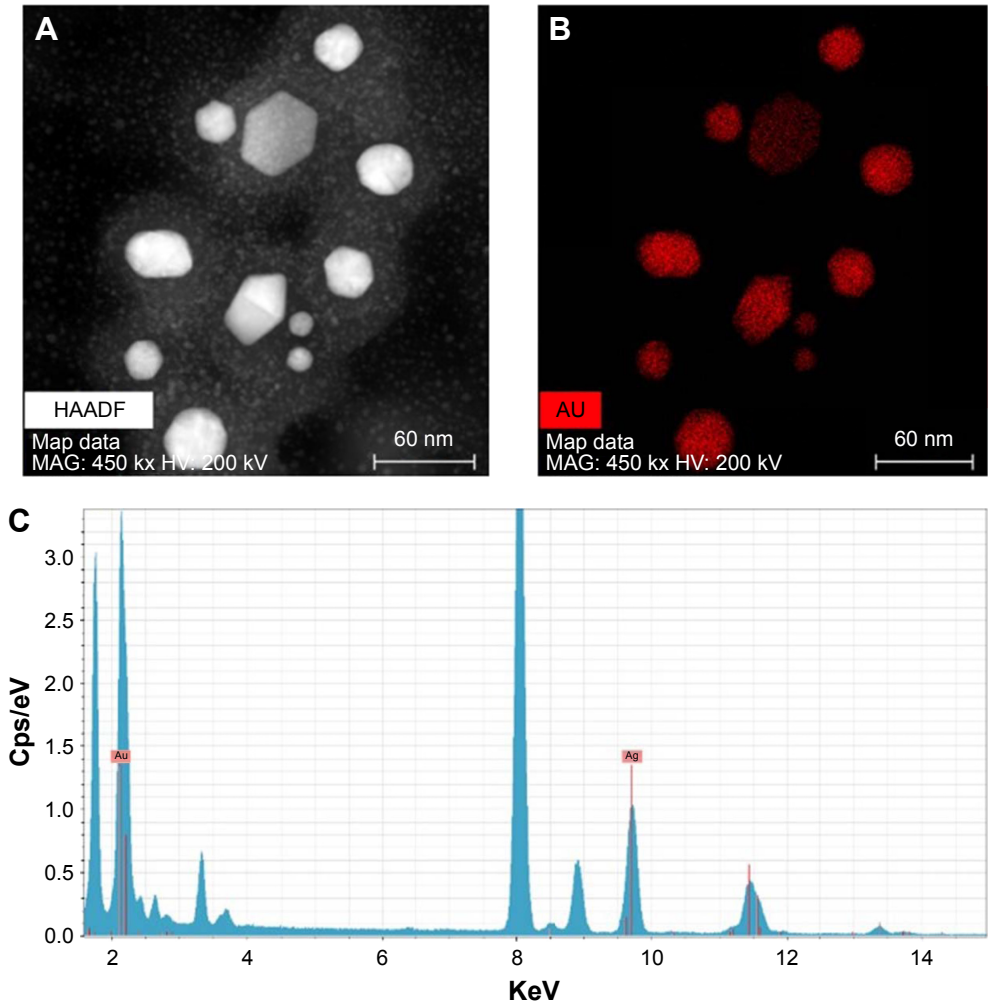

Figure 3 EDS analysis of the synthesized KC-GNs.
Notes: (**A** and **B**) KC-GNs showed the maximum distribution of gold elements in the corresponding nanoparticles. (**C**) The EDS spectrum of KC-GNs confirmed the presence of the characteristic peak of metallic gold.
Abbreviations: EDS, energy-dispersive X-ray spectrometry; KC-GN, Kalopanacis Cortex extract-capped gold nanoparticle; CPS, count rate.

was conducted for 8 h (optimal standard duration) to stimulate SH-SY5Y cell injury in subsequent bioassays. Next, we evaluated the cytotoxicity of KC-GNs for SH-SY5Y cells using the MTT and LDH assays to determine appropriate in vitro treatment doses. The activity and effects of KC-GNs were compared with those of GNPs synthesized with sodium citrate (ci-GNs). As shown in Figure 5C and D, no notable cell toxicity was detected after treatment with KC-GNs at concentrations <200 μg/mL. In addition, the viability of SH-SY5Y cells was not affected by the treatment with ci-GNs up to 100 μg/mL (data not shown). Therefore, a concentration of 100 μg/mL ci-GNs and KC-GNs was used for subsequent experiments. We tested the potential effects of ci-GNs and KC-GNs against OGD/R-induced cell injury. The MTT and LDH assays demonstrated that OGD/R induced significant cytotoxicity for SH-SY5Y cells, which was significantly alleviated by KC-GNs but only weakly attenuated by ci-GNs (Figure 5E and F). Moreover, the OGD/R-induced damage caused morphological changes in SH-SY5Y cells, resulting in a round and shrunken appearance (Figure 5G). The treatment with KC-GNs during OGD/R markedly attenuated the morphological damage to SH-SY5Y cells, which was only weakly attenuated by ci-GNs. These observations were in accordance with the results of the MTT and LDH assays.

KC-GNs prevented OGD/R-induced apoptosis of human neuronal cells

To determine whether KC-GNs could prevent the OGD/R-induced apoptosis, we used the TUNEL assay with SH-SY5Y cells. The TUNEL stain was used to evaluate the percentage of cells undergoing apoptosis. As shown in Figure 6A and B, the percentage of TUNEL-positive cells significantly increased after exposure to OGD/R compared with that observed under normoxic conditions. However,

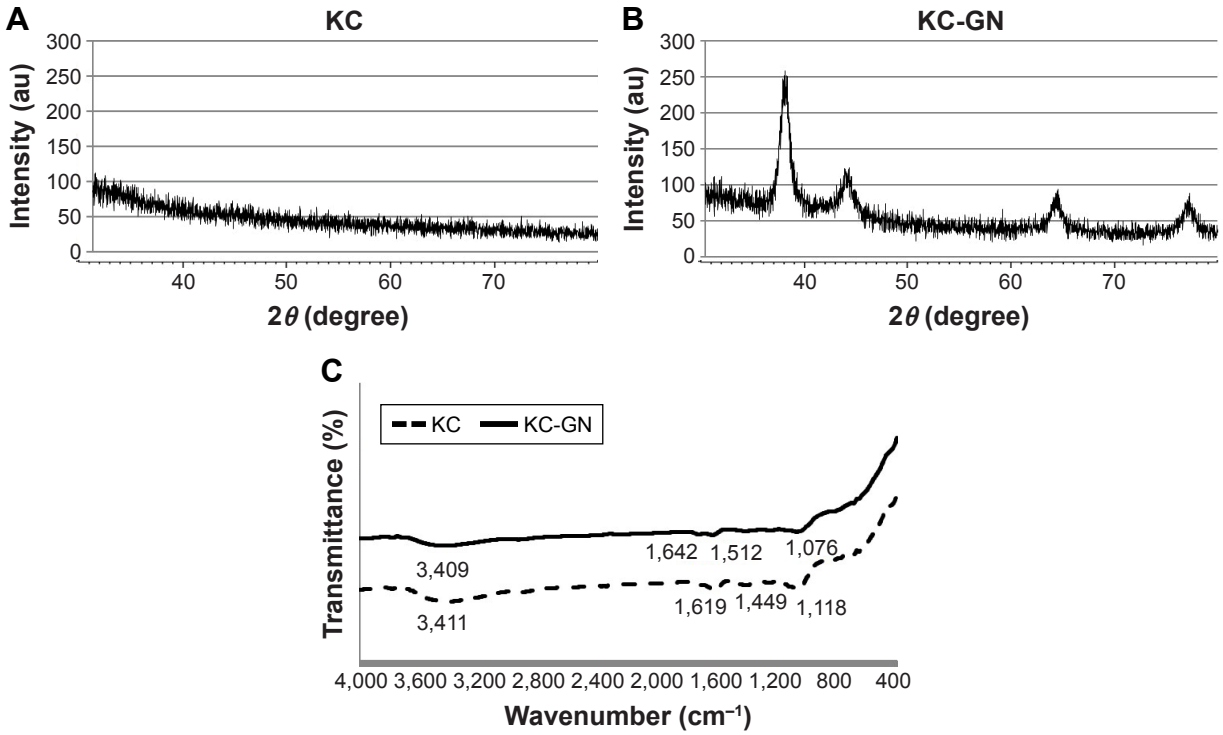

Figure 4 Structural analysis of synthesized KC-GNs.
Notes: (**A** and **B**) XRD patterns of the KC extract and synthesized KC-GNs. (**C**) FTIR spectra of the KC extract and synthesized KC-GNs.
Abbreviations: FTIR, Fourier transform infrared; KC, Kalopanacis Cortex; KC-GN, Kalopanacis Cortex extract-capped gold nanoparticle; XRD, X-ray diffraction.

pretreatment with KC-GNs markedly reduced the number of TUNEL-positive cells compared with that observed in response to OGD/R treatment, while ci-GNs only slightly reduced the number of TUNEL-positive cells. In addition, we investigated the expression of proteins that are considered reliable apoptosis-related markers (cleaved caspase-3, p53, p21, and B-cell lymphoma 2-associated X protein [Bax]) to assess the apoptosis of OGD/R-induced cells. The expression levels of cleaved caspase-3, p53, p21, and Bax proteins were significantly increased by the treatment with OGD/R compared with those observed under normoxia. Our data showed that KC-GNs inhibited the overexpression of the apoptosis-related markers induced by OGD/R (Figure 6C). We also examined the activity of cleaved caspase-3 using immunofluorescence analysis and found that KC-GNs significantly decreased the cleaved caspase-3 activity in OGD/R-induced cells (Figure 6D).

Attenuation of OGD/R-induced elevation of ROS production and mitochondrial dysfunction by KC-GNs

Oxidative stress is thought to be central to the pathology of ischemic injury and is an early event in neuronal cells exposed to OGD/R.[5] Intracellular ROS was detected by flow cytometric analysis, which demonstrated that ROS production was markedly increased after exposure to OGD/R but was inhibited by KC-GNs (Figure 7A and B). These results suggested that KC-GNs have antioxidant properties. Furthermore, it has been reported that mitochondrial dysfunction is an early event in OGD/R-exposed neuronal cells. Therefore, we used flow cytometric analysis with the 5,5′,6,6′-tetrachloro-1,1′,3,3′-tetraethylbenzimidazolylcarbocyanine chloride (JC-1) dye to assess mitochondrial dysfunction. The staining indicated that KC-GNs attenuated the OGD/R-induced depolarization of mitochondrial membranes (Figure 7C and D), while ci-GNs only weakly inhibited membrane depolarization.

KC-GN-mediated antioxidant effects were associated with the NRF2 signaling pathway

The NRF2 signaling pathway regulates the expression of antioxidant Phase II enzymes and contributes to the endogenous protection against oxidative stress caused by ischemic injury.[12] To investigate the underlying mechanism by which KC-GNs mediated antioxidative effects, we determined the distribution of NRF2 by immunofluorescence analysis. Our results revealed that under normoxic conditions or OGD/R,

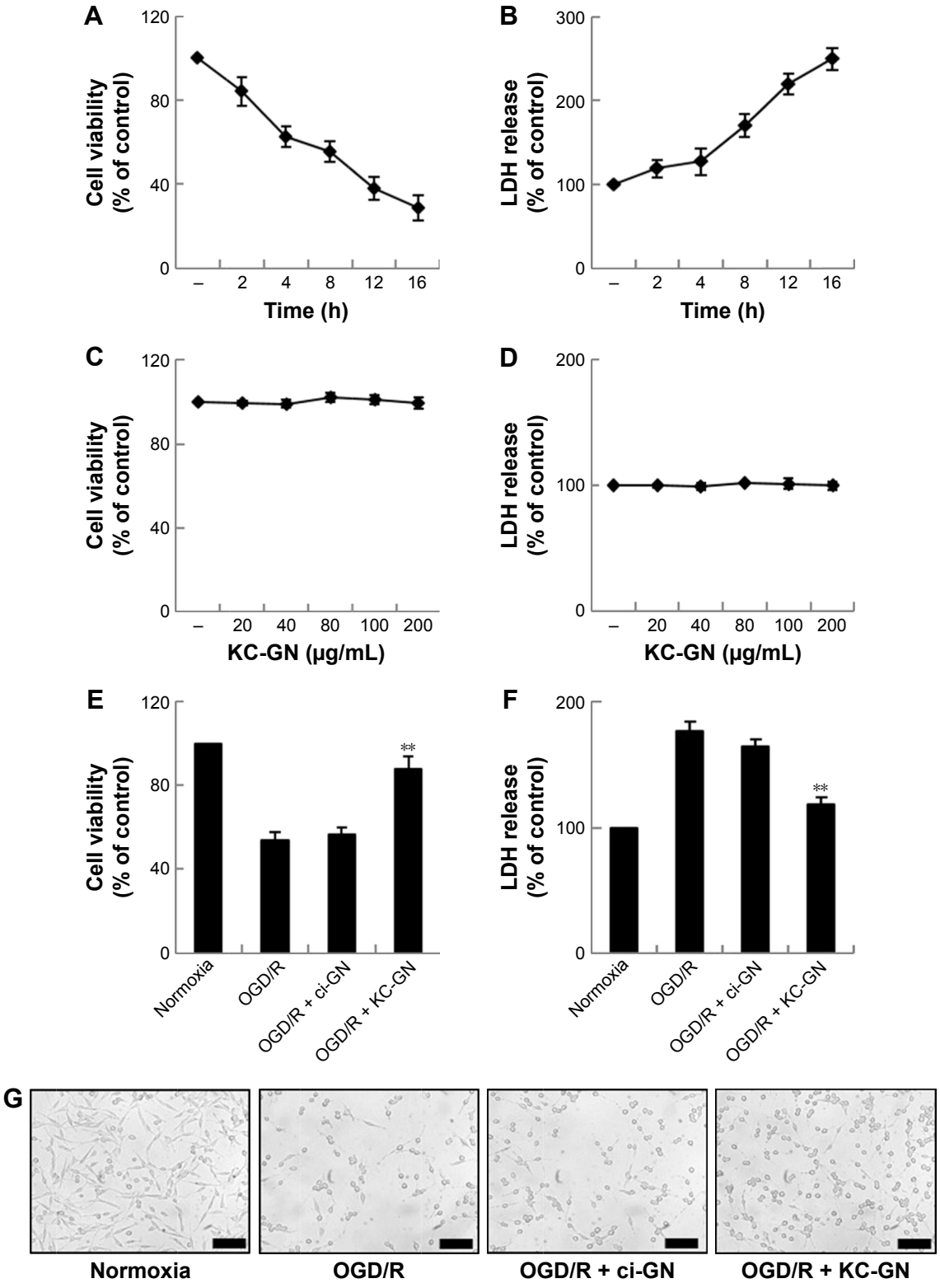

Figure 5 Neuroprotective effects of KC-GNs against OGD/R-induced cytotoxicity in human neuronal SH-SY5Y cells.

Notes: (**A** and **B**) SH-SY5Y cells were exposed to a time course of OGD, and the reoxygenation period was always 24 h. (**A**) Cell viability was analyzed using the MTT assay. (**B**) Cytotoxicity was determined using the LDH assay. (**C** and **D**) Cells were treated with different concentrations of KC-GNs for 48 h, and cell viability was assessed by the MTT (**C**) and LDH (**D**) assays. (**E** and **F**) Cells were pretreated with 100 μg/mL KC-GNs or ci-GNs for 1 h and then exposed to OGD for 8 h and reoxygenated for a further 24 h. The cell viability was assessed by the MTT (**E**) and LDH (**F**) assays. (**G**) Cell morphology was evaluated with phase-contrast microscopy. Each bar represents the mean ± standard error of three independent experiments per group. $^{**}P<0.01$ relative to the OGD/R-treated group.

Abbreviations: ci-GN, sodium citrate–gold nanoparticle; KC-GN, Kalopanacis Cortex extract-capped gold nanoparticle; LDH, lactate dehydrogenase; MTT, 3-(4,5-dimethylthiazol-2-yl)-2,5-diphenyltetrazolium bromide; OGD/R, oxygen–glucose deprivation/reoxygenation.

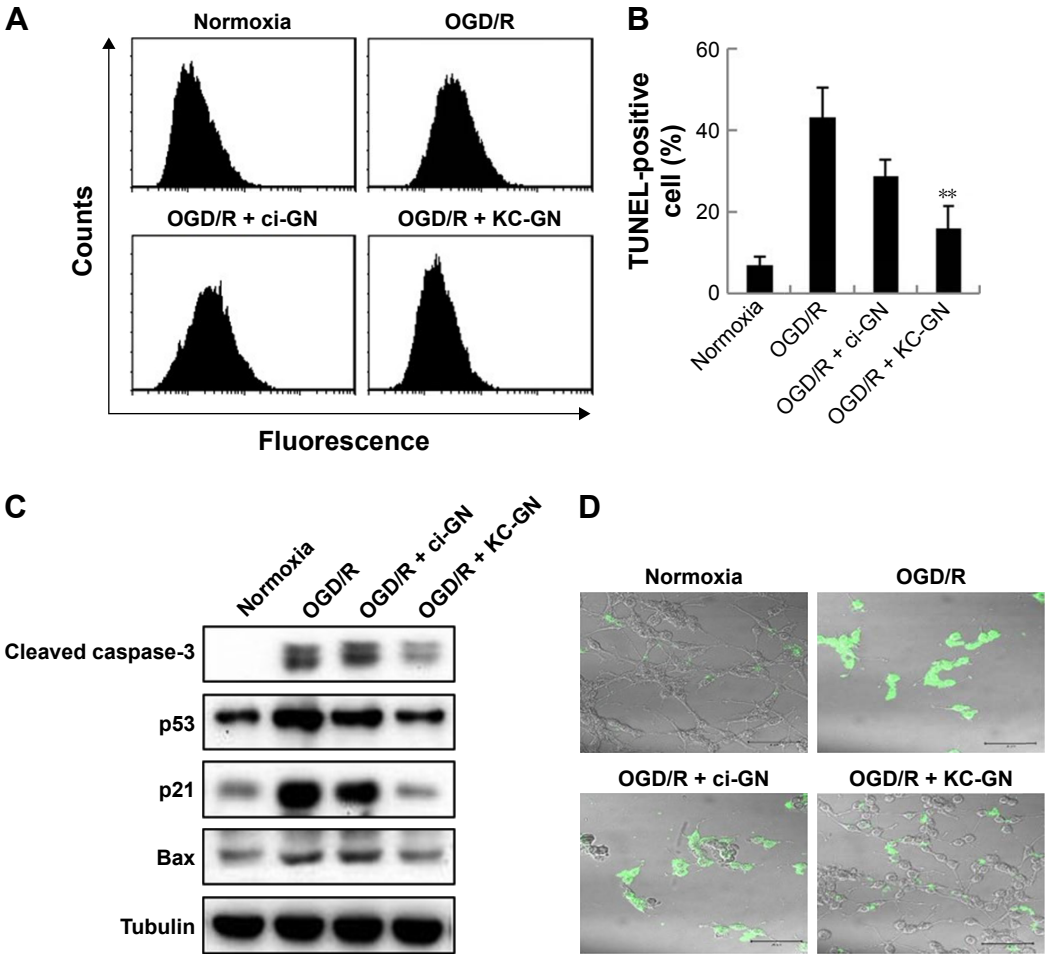

Figure 6 KC-GNs inhibited the OGD/R-induced apoptosis in human neuronal SH-SY5Y cells.

Notes: Cells were pretreated with 100 μg/mL KC-GNs or ci-GNs for 1 h and then maintained under OGD for 8 h and reoxygenated for 24 h. (**A**) Cellular apoptosis was detected by the TUNEL assay. (**B**) The fluorescence intensity of the TUNEL stain in cells was compared between groups. (**C**) Effects of KC-GNs and ci-GNs on the protein expression of cleaved caspase-3, p53, p21, and Bax in cells exposed to OGD/R. Tubulin was used as an internal control to normalize the data. (**D**) Representative confocal microscopic images of OGD/R-stimulated cells treated with KC-GNs or ci-GNs, obtained using a cleaved caspase-3–Alexa Fluor 488 antibody conjugate (green fluorescence). Scale bar =50 μm. Each bar represents the mean ± standard error of three independent experiments per group. $^{**}P<0.01$ relative to the OGD/R-treated group.

Abbreviations: Bax, B-cell lymphoma 2-associated X protein; ci-GN, sodium citrate–gold nanoparticle; KC-GN, Kalopanacis Cortex extract-capped gold nanoparticle; OGD/R, oxygen–glucose deprivation/reoxygenation; TUNEL, terminal deoxynucleotidyl transferase dUTP nick end labeling.

NRF2 was predominantly distributed in the cytoplasm. However, after treatment with KC-GNs, NRF2 translocated from the cytoplasm to the nucleus in OGD/R-induced cells (Figure 8A). To further confirm the targeted relationship between KC-GNs and NRF2, nuclear accumulation of NRF2 was investigated by Western blot analysis. The results showed that KC-GNs significantly increased the nuclear accumulation of NRF2 in cells stimulated with OGD/R (Figure 8B). To confirm the regulatory effect of KC-GNs on NRF2 signaling, we examined the effect of KC-GNs on downstream signaling of NRF2. The luciferase reporter assay indicated that KC-GNs significantly increased the ARE activity in SH-SY5Y cells exposed to OGD/R (Figure 8C). Moreover, expression of the target genes, *HO-1* and *NQO1*, was also markedly upregulated by KC-GNs in SH-SY5Y cells exposed to OGD/R (Figure 8D and E). These results indicated that KC-GNs stimulated the NRF2/ARE signaling pathway.

Neuroprotective effect of KC-GNs against OGD-induced injury was mediated through NRF2 signaling

To verify whether KC-GNs protected human neuronal cells from OGD/R via NRF2 signaling, we silenced the expression of NRF2 or HO-1 and then treated cells with KC-GNs. The inhibitory effects of KC-GNs on OGD/R-induced cytotoxicity and apoptosis (Figure 9A) and ROS production (Figure 9B) were significantly reversed by NRF2 or HO-1 silencing. Collectively, these data indicated that KC-GNs

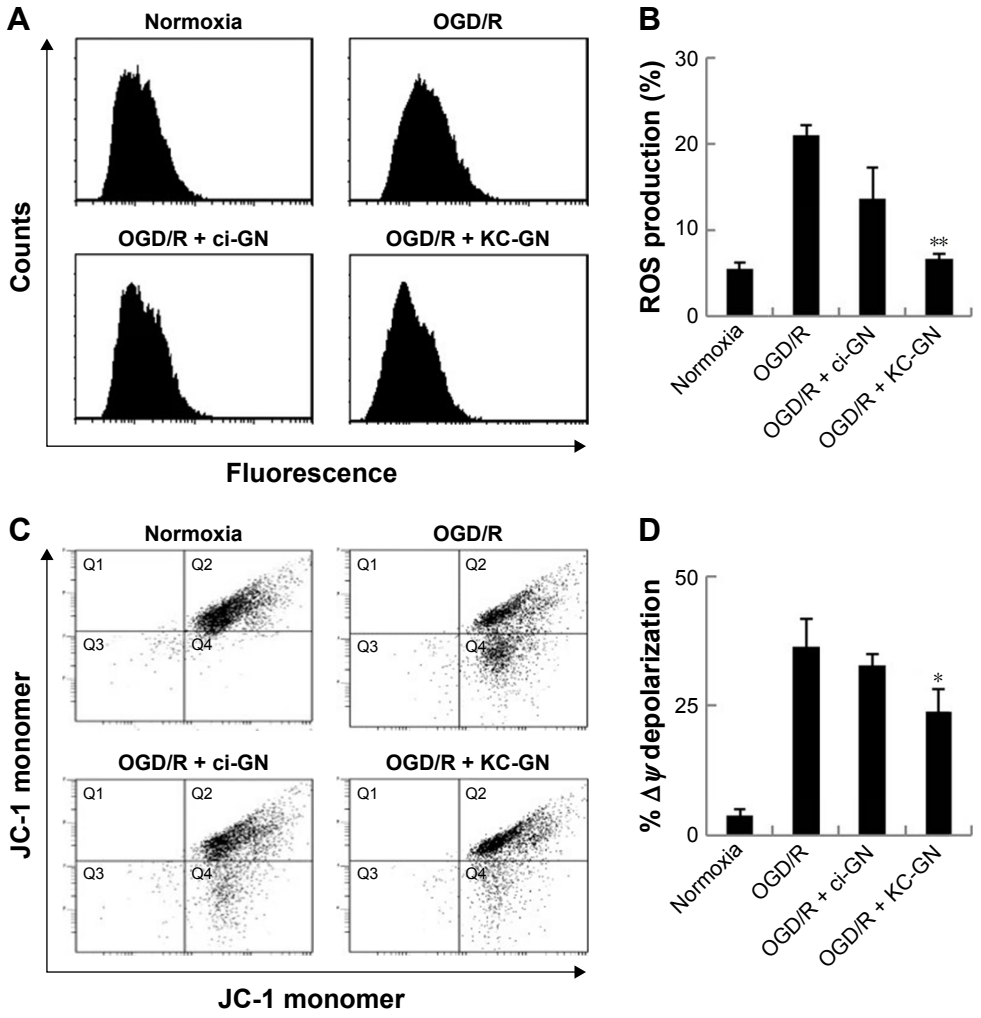

Figure 7 Effects of KC-GNs on ROS production and mitochondrial dysfunction in OGD/R-induced SH-SY5Y cells.
Notes: Cells were treated with KC-GNs or ci-GNs for 1 h and then exposed to OGD/R. (**A**) CM-H_2DCFDA (a general oxidative stress indicator) was used to measure the level of intracellular ROS production. (**B**) Fluorescence intensity was measured by flow cytometry to determine the intracellular ROS level. (**C**) Cells were stained with the JC-1 dye as a mitochondrial membrane potential indicator and analyzed by flow cytometry. (**D**) The indicated percentage of cells in the lower right quadrant emitted only green fluorescence, which was attributed to depolarized mitochondrial membranes. Each bar represents the mean ± standard error of three independent experiments per group. *$P<0.05$ and **$P<0.01$ relative to the OGD/R-treated group.
Abbreviations: ci-GN, sodium citrate–gold nanoparticle; CM-H_2DCFDA, chloromethyl derivative of 2′,7′-dichlorodihydrofluorescein diacetate; JC-1, 5,5′,6,6′-tetrachloro-1,1′,3,3′-tetraethyl-benzimidazolylcarbocyanine chloride; KC-GN, Kalopanacis Cortex extract-capped gold nanoparticle; OGD/R, oxygen–glucose deprivation/reoxygenation; ROS, reactive oxygen species.

protected human neuronal cells against OGD/R injury through NRF2 signaling.

Discussion

Recently, medicinal plants have been proposed as an inexpensive and reliable source of green reducing agents for use in the metal-based nanotechnology.[26] In particular, biotechnological synthesis of GNPs using medicinal plant extracts has attracted attention in the biomedical field. Medicinal plant extracts are being increasingly used for the preparation of magnetically recoverable gold in order to develop green synthesis methods.[27] Methods used in green synthesis of GNPs with medicinal plant extracts are characterized as eco-friendly, single step, safe, and cost-effective.[28,29] Since gold exhibits little or no toxicity to animal cells, GNPs such as KC-GNs may offer beneficial effects in the development of more potent agents against ischemic injury. First, we synthesized GNPs using a KC extract, which can efficiently catalyze natural transformations under heterogeneous conditions. A single-step and rapid synthesis (within 10–15 min) of stable, spherical GNPs (25–40 nm) was achieved with the KC extract.

Characterization of KC-GNs was conducted using UV–Vis spectroscopy, DLS, HR-TEM, EDS, XRD, and FTIR analyses. These methods were used to obtain different characteristics, such as the particle size, particle nature,

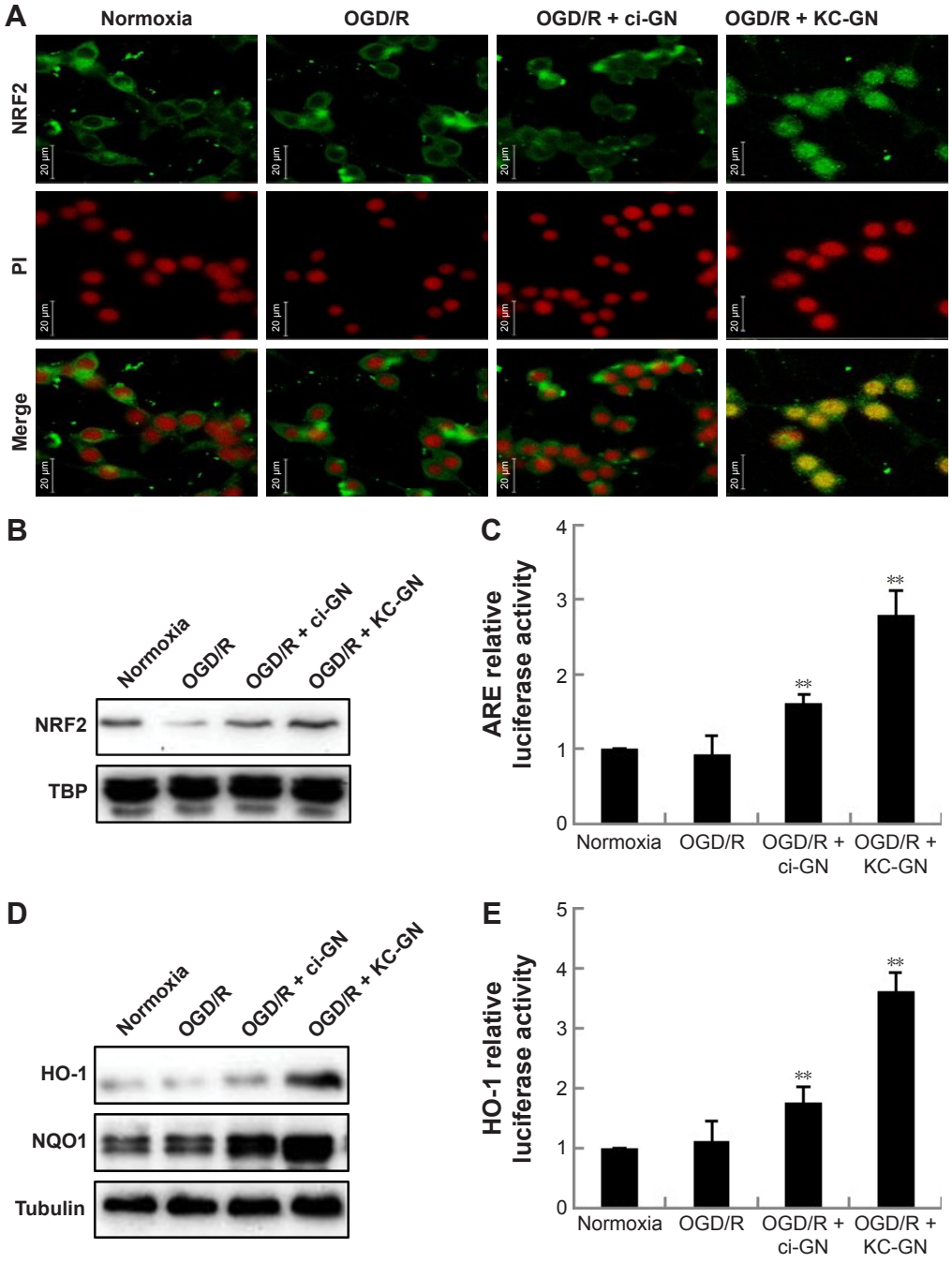

Figure 8 KC-GNs activate NRF2/ARE signaling and induce the expression of HO-1 and NQO1.

Notes: Cells were pretreated with KC-GNs or ci-GNs for 1 h before OGD/R treatment. (**A**) Fixed cells were stained with PI and an anti-NRF2 antibody, followed by incubation with an FITC-conjugated anti-rabbit IgG secondary antibody. The samples were observed by confocal microscopy. Scale bar =20 μm. (**B**) Western blot was used to detect the NRF2 protein, with TBP used as the internal control. (**C**) Cells transfected with the ARE–luciferase reporter plasmid were incubated with KC-GNs for 1 h and then exposed to OGD/R. Equal amounts of the cell extract were assayed for dual-luciferase activity. (**D**) Expression of the HO-1 and NQO1 proteins was examined by Western blot. (**E**) Cells were transfected with the HO-1 promoter reporter plasmid. Each bar represents the mean ± standard error of three independent experiments per group. $^{**}P<0.01$ relative to the OGD/R-treated group.

Abbreviations: ARE, antioxidant response element; ci-GN, sodium citrate–gold nanoparticle; FITC, fluorescein isothiocyanate; HO-1, heme oxygenase-1; KC-GN, Kalopanacis Cortex extract-capped gold nanoparticle; NQO1, NAD(P)H quinone dehydrogenase 1; NRF2, nuclear factor erythroid 2-related factor 2; OGD/R, oxygen–glucose deprivation/reoxygenation; PI, propidium iodide; TBP, TATA-binding protein.

crystallinity, surface area, and overall characteristics. Typically, GNPs show characteristic SPR phenomena at wavelengths in the range from 520 to 545 nm, which was also observed for KC-GNs as a high absorbance value at 527 nm. The DLS and zeta potential results indicated that the average diameter of KC-GNs was 54.02±2.19 nm, and the apparent zeta potential was −20.3±0.04 mV. Zeta potential was used to study the surface charges and stability of KC-GNs. The

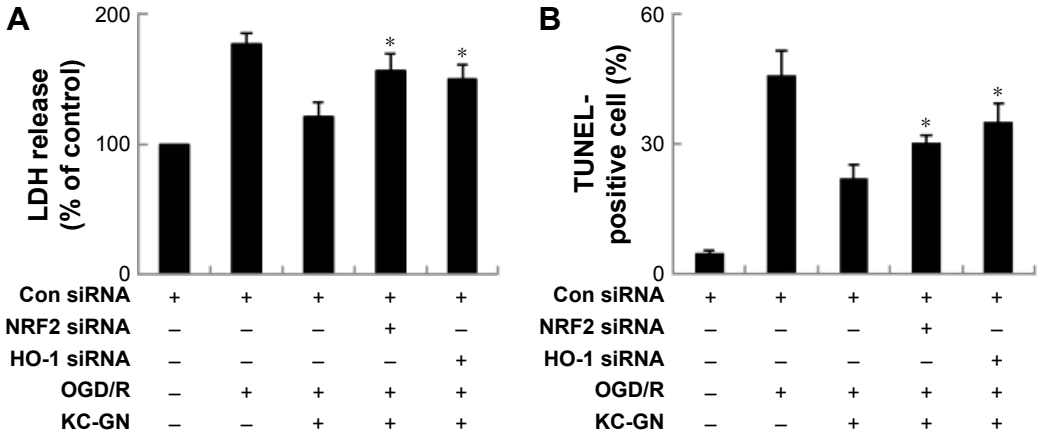

Figure 9 NRF2 signal silencing eliminates the protective effects of KC-GNs.
Notes: Cells were transfected with the control siRNA and siRNA targeting NRF2 or HO-1. In all, 24 h after the transfection, cells were treated with KC-GNs for 1 h and then treated with OGD/R, followed by the LDH assay (**A**) and the TUNEL assay (**B**). *$P<0.05$ relative to the OGD/R-treated group.
Abbreviations: HO-1, heme oxygenase-1; KC-GN, Kalopanacis Cortex extract-capped gold nanoparticle; LDH, lactate dehydrogenase; NRF2, nuclear factor erythroid 2-related factor 2; OGD/R, oxygen–glucose deprivation/reoxygenation; siRNA, small interfering RNA; TUNEL, terminal deoxynucleotidyl transferase dUTP nick end labeling.

surface charge could greatly influence the particle size distribution and cellular uptake of KC-GNs. The DLS results demonstrated that KC-GNs were small and stable and showed no obvious aggregation. The surface morphology of KC-GNs was observed by HR-TEM, and the elemental composition was analyzed by EDS. As shown by the EDS pattern, KC-GNs were crystalline in nature, which affected the reduction of gold ions. The nature of the synthesized KC-GNs, analyzed by XRD, showed that the four diffraction peaks corresponded to the (111), (200), (220), and (311) planes of gold, respectively, as the bands for the FCC structure of gold. This characteristic structural pattern confirmed that KC-GNs had a crystalline structure. The intense peak in the FTIR spectra observed at 3,411 cm^{-1} corresponded to O–H stretching; those observed at 1,619 and 1,449 cm^{-1} corresponded to C–C stretching of aromatic groups, and that at 1,076 cm^{-1} corresponded to C–N stretching of aliphatic amine groups in the KC extract, which was used as a reducing, capping, and stabilizing agent for the synthesis of KC-GNs. The slight shifts in the positions of the four peaks in KC-GNs compared to those in the KC extract might have occurred because of the reduction reaction upon capping and stabilization of KC-GNs by various bioactive compounds present in KC.

Although metal nanoparticles are an emerging focus of diagnostics and therapy against neurodegenerative diseases, particularly with respect to their properties and applications,[30] few studies have focused on the impact of green synthesis of GNPs on their neuroprotective properties. Therefore, the protective properties of KC-GNs against neurodegenerative diseases could be useful in the development of new antineurodegenerative treatments against ischemic injury. We examined the neuroprotective effect of KC-GNs on human neuronal SH-SY5Y cells with OGD/R-induced damage and demonstrated that the molecular mechanism of KC-GNs involved NRF2 signaling. OGD/R is a well-established neuronal cellular injury model, which mimics the in vivo variations that occur after an ischemic insult, and human neuronal SH-SY5Y cells are sensitive to ischemic injury. Many studies have established that OGD/R leads to obvious cell morphological changes, decreased cell survival, increased ROS production, and mitochondrial dysfunction. Our results obtained using OGD/R-treated SH-SY5Y cells showed similar effects. SH-SY5Y cells showed a significant decrease in viability, as evidenced by the MTT and LDH assay results. However, we observed that KC-GNs effectively attenuated the OGD/R-induced neuronal cell death. Similarly, the OGD-induced LDH release was reduced by KC-GNs, which further supported the protective effect of KC-GN against OGD/R-induced cytotoxicity. Currently, the apoptosis pathway in injured neural cells is known to feature the activation of DNA fragmentation (measured by the TUNEL assay) and caspase-3, as well as the upregulation of p53, the cyclin-dependent kinase inhibitor p21, and the pro-apoptotic protein Bax. Our study also indicated that pretreatment with KC-GNs decreased the OGD/R-induced TUNEL and caspase-3 activity, as well as the upregulation of p53, p21, and Bax expression in SH-SY5Y cells, which suggested that KC-GNs protected against the OGD/R-induced injury by inhibition of apoptosis.

Ischemic injury results in the massive production of ROS, which directly damages main cellular components. Additionally, the restoration of oxygen levels in hypoxic tissues

stimulates ROS production.[31,32] Because of their fragile cell membrane lipid layers and low levels of antioxidant enzymes, neuronal cells are extremely sensitive to oxidative stress. In our study, KC-GNs significantly decreased the OGD/R-induced ROS production, which implies that KC-GNs alleviated the OGD/R-induced oxidative stress. Mitochondria, which are OGD/R-sensitive organelles, play an essential role in ischemic injury, and our results also showed that the mitochondrial membrane potential was improved by KC-GN treatment. KC-GNs also ameliorated mitochondrial dysfunction. Some functional groups from the KC extract were incorporated into KC-GNs, which provided stability and enhanced neuroprotective properties of GNPs. Moreover, our data suggested that in comparison with ci-GNs, KC-GNs showed stronger neuroprotective properties against OGD/R treatment. Consequently, cells pretreated with KC-GNs showed greater protection against OGD/R in the cytotoxicity, apoptosis, oxidative stress, and mitochondrial dysfunction assays.

At the molecular level, these effects of KC-GNs under conditions of OGD/R can be explained by the induction of a neuroprotective mechanism, which specifically targets the NRF2/ARE signaling pathway. Neuroprotective properties are mediated primarily by a group of evolutionarily conserved transcription factors, known as the NRF2 signaling pathway, and activation of NRF2/ARE-regulated genes in neuronal cells results in more efficient detoxification, antioxidant defense, and endogenous cellular protection. Hence, NRF2 activation in neuronal cells has been proposed as a novel therapeutic strategy for neuroprotection.[9,11] Our results indicated that under unstressed conditions, KC-GNs showed almost no effect on the activity of NRF2 in cells (data not shown). However, the nuclear accumulation of NRF2 increased in OGD/R-treated cells after KC-GN treatment compared with that in cells only treated with OGD/R, which suggested that KC-GNs might exert antioxidant and detoxifying effects in response to certain neurotoxic conditions. KC-GNs induced an increase in the expression of

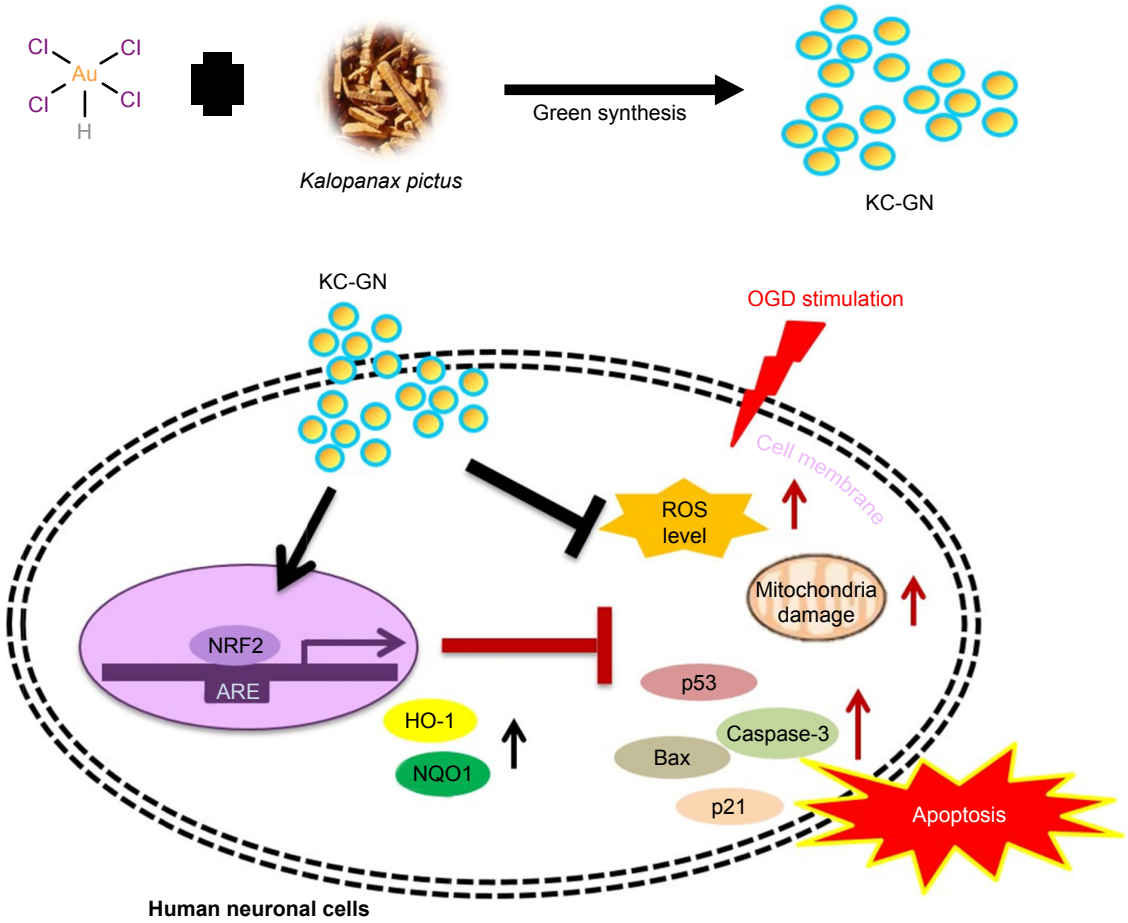

Figure 10 Scheme illustrating the neuroprotective properties of KC-GNs against OGD-induced injury in human neuronal cells.
Abbreviations: ARE, antioxidant response element; HO-1, heme oxygenase-1; KC-GN, Kalopanacis Cortex extract-capped gold nanoparticle; NQO1, NAD(P)H quinone dehydrogenase 1; NRF2, nuclear factor erythroid 2-related factor 2; OGD, oxygen–glucose deprivation/reoxygenation; ROS, reactive oxygen species.

NRF2-mediated genes, including those encoding HO-1 and NQO1, in OGD/R-treated cells. Importantly, the neuroprotective properties of KC-GNs were blocked when the NRF2 expression was reduced with siRNA specifically targeting NRF2 or HO-1, which suggested that KC-GN-mediated neuroprotection may occur through NRF2/ARE signaling.

Limitations of the study

Applications of metal nanoparticles in clinical neuroscience are in the initial stages of development, partly because of the complexity of the central nervous system. Although the attention to the application of metal nanoparticles in neuroprotection is increasing, clinical studies are still limited because of the lack of knowledge about the consequences of GNPs as neuroprotective agents against ischemic stroke. Furthermore, many of the cellular and molecular signal mechanisms of neuroprotective responses and GNP–neuronal interactions are not yet well understood. Finally, the results of this in vitro study need to be confirmed in an in vivo model of ischemic stroke, which will be the focus of ongoing studies.

Conclusion

A novel, eco-friendly, simple, and inexpensive synthesis of KC-GNs was reported using a KC extract. The intrinsic bioactive compounds of KC acted as reducing, capping, and stabilizing agents, which therefore excluded the need to use toxic chemicals. The synthesized KC-GNs were characterized by a variety of standard analytical techniques. This study provided the first experimental evidence that KC-GNs induced the activation of NRF2/ARE in human neuronal cells and provided a neuroprotective effect against OGD/R stimulation (Figure 10). Collectively, our results revealed that KC-GNs provided neuroprotection via NRF2/ARE signaling and suggested a promising therapeutic strategy for ischemic stroke.

Acknowledgment

This research was supported by the Basic Science Research Program through the National Research Foundation of Korea (NRF), which was funded by the Ministry of Education, Science, and Technology (2015R1D1A1A01059450).

Disclosure

The authors report no conflicts of interest in this work.

References

1. Yu CZ, Li C, Pei DS, et al. Neuroprotection against transient focal cerebral ischemia and oxygen-glucose deprivation by interference with GluR6-PSD95 protein interaction. *Neurochem Res*. 2009;34(11):2008–2021.
2. Bak SW, Choi H, Park HH, et al. Neuroprotective effects of acetyl-L-carnitine against oxygen-glucose deprivation-induced neural stem cell death. *Mol Neurobiol*. 2016;53(10):6644–6652.
3. Aueviriyavit S, Phummiratch D, Maniratanachote R. Mechanistic study on the biological effects of silver and gold nanoparticles in Caco-2 cells – induction of the Nrf2/HO-1 pathway by high concentrations of silver nanoparticles. *Toxicol Lett*. 2014;224(1):73–83.
4. Guo H, Kong S, Chen W, et al. Apigenin mediated protection of OGD-evoked neuron-like injury in differentiated PC12 cells. *Neurochem Res*. 2014;39(11):2197–2210.
5. Sun LP, Xu X, Hwang HH, Wang X, Su KY, Chen YL. Dichloromethane extracts of propolis protect cell from oxygen-glucose deprivation-induced oxidative stress via reducing apoptosis. *Food Nutr Res*. 2016; 60:30081.
6. He G, Xu W, Tong L, et al. Gadd45b prevents autophagy and apoptosis against rat cerebral neuron oxygen-glucose deprivation/reperfusion injury. *Apoptosis*. 2016;21(4):390–403.
7. Nie H, Xue X, Li J, et al. Nitro-oleic acid attenuates OGD/R-triggered apoptosis in renal tubular cells via inhibition of Bax mitochondrial translocation in a PPAR-gamma-dependent manner. *Cell Physiol Biochem*. 2015;35(3):1201–1218.
8. Gu DM, Lu PH, Zhang K, et al. EGFR mediates astragaloside IV-induced Nrf2 activation to protect cortical neurons against in vitro ischemia/reperfusion damages. *Biochem Biophys Res Commun*. 2015;457(3): 391–397.
9. Chen X, Liu Y, Zhu J, et al. GSK-3beta downregulates Nrf2 in cultured cortical neurons and in a rat model of cerebral ischemia-reperfusion. *Sci Rep*. 2016;6:20196.
10. Shen C, Cheng W, Yu P, et al. Resveratrol pretreatment attenuates injury and promotes proliferation of neural stem cells following oxygen-glucose deprivation/reoxygenation by upregulating the expression of Nrf2, HO-1 and NQO1 in vitro. *Mol Med Rep*. 2016;14(4): 3646–3654.
11. Meng X, Wang M, Wang X, et al. Suppression of NADPH oxidase- and mitochondrion-derived superoxide by Notoginsenoside R1 protects against cerebral ischemia-reperfusion injury through estrogen receptor-dependent activation of Akt/Nrf2 pathways. *Free Radic Res*. 2014; 48(7):823–838.
12. Xu XH, Li GL, Wang BA, et al. Diallyl trisufide protects against oxygen glucose deprivation-induced apoptosis by scavenging free radicals via the PI3K/Akt-mediated Nrf2/HO-1 signaling pathway in B35 neural cells. *Brain Res*. 2015;1614:38–50.
13. Lai TH, Shieh JM, Tsou CJ, Wu WB. Gold nanoparticles induce heme oxygenase-1 expression through Nrf2 activation and Bach1 export in human vascular endothelial cells. *Int J Nanomedicine*. 2015;10: 5925–5939.
14. Goldstein A, Soroka Y, Frusic-Zlotkin M, Lewis A, Kohen R. The bright side of plasmonic gold nanoparticles; activation of Nrf2, the cellular protective pathway. *Nanoscale*. 2016;8(22):11748–11759.
15. Xu MX, Wang M, Yang WW. Gold-quercetin nanoparticles prevent metabolic endotoxemia-induced kidney injury by regulating TLR4/NF-kappaB signaling and Nrf2 pathway in high fat diet fed mice. *Int J Nanomedicine*. 2017;12:327–345.
16. Gurunathan S, Han J, Park JH, Kim JH. A green chemistry approach for synthesizing biocompatible gold nanoparticles. *Nanoscale Res Lett*. 2014;9(1):248.
17. Mukherjee S, Sau S, Madhuri D, et al. Green synthesis and characterization of monodispersed gold nanoparticles: toxicity study, delivery of doxorubicin and its bio-distribution in mouse model. *J Biomed Nanotechnol*. 2016;12(1):165–181.
18. Kumar CG, Poornachandra Y, Mamidyala SK. Green synthesis of bacterial gold nanoparticles conjugated to resveratrol as delivery vehicles. *Colloids Surf B Biointerfaces*. 2014;123:311–317.
19. Hwang SJ, Jun SH, Park Y, et al. Green synthesis of gold nanoparticles using chlorogenic acid and their enhanced performance for inflammation. *Nanomedicine*. 2015;11(7):1677–1688.

20. Patra JK, Baek KH. Comparative study of proteasome inhibitory, synergistic antibacterial, synergistic anticandidal, and antioxidant activities of gold nanoparticles biosynthesized using fruit waste materials. *Int J Nanomedicine*. 2016;11:4691–4705.
21. Harikrishnan R, Kim JS, Kim MC, Balasundaram C, Heo MS. Kalopanax pictus as feed additive controls bacterial and parasitic infections in kelp grouper, *Epinephelus bruneus*. *Fish Shellfish Immunol*. 2011;31(6):801–807.
22. Jeong YH, Hyun JW, Kim Van Le T, Kim DH, Kim HS. Kalopanax-saponin A exerts anti-inflammatory effects in lipopolysaccharide-stimulated microglia via inhibition of JNK and NF-kappaB/AP-1 pathways. *Biomol Ther (Seoul)*. 2013;21(5):332–337.
23. Bang SY, Park GY, Park SY, et al. The stem bark of *Kalopanax pictus* exhibits anti-inflammatory effect through heme oxygenase-1 induction and NF-kappaB suppression. *Immune Netw*. 2010;10(6):212–218.
24. Quang TH, Ngan NT, Minh CV, et al. Effect of triterpenes and triterpene saponins from the stem bark of *Kalopanax pictus* on the transactivational activities of three PPAR subtypes. *Carbohydr Res*. 2011;346(16):2567–2575.
25. Ahmed S, Annu, Ikram S, Yudha SS. Biosynthesis of gold nanoparticles: a green approach. *J Photochem Photobiol B*. 2016;161:141–153.
26. Naraginti S, Kumari PL, Das RK, Sivakumar A, Patil SH, Andhalkar VV. Amelioration of excision wounds by topical application of green synthesized, formulated silver and gold nanoparticles in albino Wistar rats. *Mater Sci Eng C Mater Biol Appl*. 2016;62:293–300.
27. Mukherjee S, Ghosh S, Das DK, et al. Gold-conjugated green tea nanoparticles for enhanced anti-tumor activities and hepatoprotection – synthesis, characterization and in vitro evaluation. *J Nutr Biochem*. 2015;26(11):1283–1297.
28. Hoshyar R, Khayati GR, Poorgholami M, Kaykhaii M. A novel green one-step synthesis of gold nanoparticles using crocin and their anticancer activities. *J Photochem Photobiol B*. 2016;159:237–242.
29. Gamal-Eldeen AM, Moustafa D, El-Daly SM, et al. Photothermal therapy mediated by gum Arabic-conjugated gold nanoparticles suppresses liver preneoplastic lesions in mice. *J Photochem Photobiol B*. 2016;163:47–56.
30. Nethi SK, Mukherjee S, Veeriah V, Barui AK, Chatterjee S, Patra CR. Bioconjugated gold nanoparticles accelerate the growth of new blood vessels through redox signaling. *Chem Commun (Camb)*. 2014;50(92):14367–14370.
31. Tian X, Peng J, Zhong J, et al. Beta-Caryophyllene protects in vitro neurovascular unit against oxygen-glucose deprivation and re-oxygenation-induced injury. *J Neurochem*. 2016;139(5):757–768.
32. Wang J, Han D, Sun M, Feng J. Cerebral ischemic postconditioning induces autophagy inhibition and a HMGB1 secretion attenuation feedback loop to protect against ischemia reperfusion injury in an oxygen glucose deprivation cellular model. *Mol Med Rep*. 2016;14(5):4162–4172.